dipole and the relative orientation of the screw axis related molecules.

In conclusion, we have demonstrated through statistical analysis that the magnitude of the molecular dipole moment does not vary significantly between centrosymmetric ($P\bar{1}$) and noncentrosymmetric ($P1$ and $P2_1$) space groups and does not correlate with relative molecular orientations within the $P2_1$ space group. This is not to say that *local* electrostatic interactions between molecules are unimportant; such local effects as hydrogen bonding, interactions of polar groups, etc. obviously do play a significant role, along with molecular shapes, in determining packing in molecular crystals. However, the high preference for organic molecules to crystallize in one of the centrosymmetric arrangements cannot be attributed to molecular dipole–dipole interactions, and attempts to design molecular arrays based primarily on considerations of overall molecular dipole moments have, statistically speaking, a small chance of success.

Acknowledgment. Financial support of this research by the donors of the Petroleum Research Fund, administered by the American Chemical Society (J.K.W.), the Robert A. Welch Foundation (F-626 to J.K.W. and F-233 to R.E.D.), the National Science Foundation (Grant DMR-9014026 to J.K.W.), and the Advanced Research Program of the Texas Higher Education Coordinating Board (Grant 277 to J.K.W. and R.E.D.) is gratefully acknowledged.

Supplementary Material Available: Tables of entries used for each of the three space groups with dipole moments and, for $P2_1$, angles (11 pages). Ordering information is given on any current masthead page.

Hydrogen Abstraction from a Diamond Surface. Ab Initio Quantum Chemical Study with Constrained Isobutane as a Model

Michael Page*,† and Donald W. Brenner*,‡

Contribution from the Naval Research Laboratory, Washington, D.C. 20375-5000.
Received October 12, 1990

Abstract: Abstraction of terminal hydrogens on a diamond {111} surface by atomic hydrogen has been offered as the possible rate-determining elementary step in the mechanism of low-pressure diamond growth by chemical vapor deposition. We use ab initio multiconfiguration self-consistent-field methods to estimate the activation energy for this abstraction reaction. We do this by first computing features of the potential energy surface for hydrogen abstraction from gas-phase isobutane and then computing features of the potential energy surface for this same system imposing constraints that mimic those found in a diamond lattice. Our results indicate that, although 5.4 kcal/mol of the CH bond energy in isobutane is attributable to structural relaxation of the radical, most of this radical relaxation energy (4.5 kcal/mol of it) is realized even with geometric constraints similar to those in a diamond lattice. We therefore predict bonds to a diamond surface to be only about 1 kcal/mol stronger than corresponding bonds to a gas-phase tertiary-carbon atom. The effect of the geometrical constraints on the activation energy for the hydrogen abstraction reaction is even smaller: all but 0.2 kcal/mol of the gas-phase radical relaxation energy at the transition state is realized even with the imposition of lattice-type constraints. Our results therefore support the use in kinetic modeling or molecular dynamics simulations of activation energies taken from analogous gas-phase hydrocarbon reactions with little or no adjustment.

I. Introduction

Despite the substantial technological advances made over the last decade in low-pressure diamond film growth by chemical vapor deposition (CVD),[1-4] much of the underlying chemical and physical mechanism remains uncertain. The one feature that appears central to the CVD process is the presence of gas-phase atomic hydrogen. One of the roles thought to be played by the hydrogen is the creation of reactive radical sites on the growing diamond surface via hydrogen abstraction. Indeed, detailed reaction mechanisms proposed for the CVD of diamond incorporate this reaction as an important, if not rate limiting, step.[5,6] The activation energy for hydrogen abstraction is therefore an essential parameter for modeling the CVD of diamond films. Yet without the ability to isolate and measure kinetic parameters for this and other related elementary reactions, we are forced either to determine these parameters theoretically or to estimate them by analogy with related experimentally known gas-phase reactions.

Semiempirical self-consistent-field calculations of the abstraction of a surface hydrogen atom from model cluster compounds have yielded disparate results. Huang, Frenklach, and Maroncelli,[7] using the MNDO method and a model ($C_{10}H_{16}$) compound, report an activation energy of 17.4 kcal/mol for hydrogen abstraction along with a caveat that, in addition to the uncertainties inherent in the model, the barrier is likely overestimated due to incomplete optimization of the transition-state structure. More recently, Valone, Trkula, and Laia,[8] using the AM1 semiempirical method, report that no activation at all is required to abstract a hydrogen from their $C_{20}H_{35}$ model compound. While these theoretical studies may be useful for comparing contrasting mechanisms within one model compound and one electronic structure model, the direct theoretical determination of activation energies for elementary chemical reaction steps involving diamond is, for the most part, too inaccurate to be useful for modeling. This is less

† Laboratory for Computational Physics and Fluid Dynamics, Code 4410.
‡ Chemistry Division, Code 6110.

(1) DeVries, R. C. *Annu. Rev. Mater. Sci.* **1987**, *17*, 161.
(2) Angus, J. C.; Hayman, C. C. *Science* **1988**, *241*, 913.
(3) Spear, K. E. *J. Am. Ceram. Soc.* **1989**, *72*, 171.
(4) Yarbrough, W. A.; Messier, R. *Science* **1990**, *247*, 688.
(5) Frenklach, M.; Spear, K. E. *J. Mater. Res.* **1988**, *3*, 133.
(6) Harris, S. J. *Appl. Phys. Lett.* **1990**, *56*, 2298. Frenchlach, M.; Wang, M. *Phys. Rev. B* **1991**, *43*, 1520.
(7) Huang, D.; Frenklach, M.; Maroncelli, M. *J. Phys. Chem.* **1988**, *92*, 6379.
(8) Valone, S. M.; Trkula, M.; Laia, J. R. *J. Mater. Res.* **1990**, *5*, 2296.

a criticism of theoretical methods than a reflection of the stringent requirements of kinetic modeling: a few kilocalories per mole translates to an order of magnitude change in a reaction rate, even at temperatures around 1000 K.

An alternative to direct theoretical predictions of activation energies is to estimate these quantities by analogy with similar known gas-phase hydrocarbon reactions. Such an approach has been invaluable in the combustion field and has been used to estimate parameters for modeling diamond surface reactions.[6]

II. Approach

Our approach is, in a sense, a combination of these two plans. We begin with the preliminary assumption that the energetics for hydrogen abstraction from a tertiary CH bond on a diamond {111} surface is no different than it is from a tertiary CH bond in a gas-phase hydrocarbon molecule, e.g., isobutane. We then use ab initio quantum chemical methods, not to predict absolute quantities, but rather to refine this picture by focusing on how the constraints of the lattice affect the abstraction reaction. The primary difference between abstraction from isobutane and abstraction from a diamond surface is that when the tertiary hydrogen is removed from isobutane, the central carbon atom changes hybridation from sp^3 toward sp^2 with a concomitant flattening of the structure about the central carbon atom, while in diamond this radical relaxation is restricted by the surrounding lattice. The CH bond in diamond should, in effect, be strengthened by the inability of the incipient radical to fully relax toward planarity. Also, because the transition state for the abstraction reaction has partial radical character, there should be an analogous effect on the activation energy for the reaction: the activation energy should be increased by the inability of the transition state to freely relax.

To find the effect of the lattice constraints on the activation energy, we first perform ab initio multiconfiguration self-consistent-field (MCSCF) calculations on the gas-phase hydrogen abstraction

$$(CH_3)_3CH + H \rightarrow (CH_3)C^{\bullet} + H_2 \qquad (1)$$

In the gas-phase calculations, all geometrical parameters are fully optimized for the reactant, the transition state, and the products at the MCSCF level. Next, as a *worst case scenario*, we perform calculations on a hypothetical system for which no radical relaxation is allowed during any stage of the abstraction process. This we call the *bulk terminated* reaction because the *tert*-butyl skeleton is constrained to keep the near tetrahedral conformation it had in the isobutane molecule. Finally, in our calculations most germane to abstraction from a diamond surface, we allow *partial radical relaxation*: the radical carbon atom is allowed to relax in the field of the fixed structure of its neighbors. Technical details about the calculations are presented in the next section. This is followed by results for each of the gas-phase, bulk-terminated, and partially relaxed reactions.

III. Electronic Structure Calculations

a. Wave Functions. The reactant and product asymptotes on the potential energy surface for hydrogen atom abstraction from isobutane are both well described by a spin restricted doublet Hartree–Fock wave function; the unpaired electron in the two cases is on the hydrogen atom and on the central carbon atom of the *tert*-butyl radical, respectively. The Hartree–Fock wave function provides an inadequate description, however, of the transition state region of the potential energy surface for reaction 1, where one bond is being broken and another is being formed. Typical of hydrogen abstraction by radicals, the significant electronic structure changes accompanying reaction 1 are confined predominantly to three electrons and three molecular orbitals (MOs). For the reactant, these include the hydrogen atom electron and MO as well as the two electrons in the attacked CH bond of isobutane with the associated bonding and antibonding MOs. At the product side, these three electrons and MOs are the carbon radical electron and MO of *tert*-butyl as well as the electrons and bonding–antibonding pair of MOs of the hydrogen molecule.

We describe these electronic structure changes with a multiconfiguration SCF (MCSCF) wave function formed by including all possible doublet-spin configurations distributing the three *active* electrons among the three *active* MOs: a 3-*in*-3 complete active space SCF (CASSCF)[9,10] wave function. This eight-configuration MCSCF wave function provides a qualitatively correct description of the orbital changes mentioned above and allows the orbital occupation numbers to smoothly change from their reactant to their product values.

The electronic structure calculations were all performed with use of the MESA[11] system of programs on the Cray XMP-24 at the Naval Research Laboratory.

b. Basis Sets. A necessary condition for obtaining a qualitatively correct description of the transition-state region for an abstraction reaction is that the overall reaction energy—energy difference between reactants and products—be reasonably well reproduced. We choose the basis set for our MCSCF calculations of the reaction based on examining the basis set dependence of the reaction energy at the Hartree–Fock level of theory.

The basis sets we examine, in various combinations on the atoms, are the STO-3G minimal basis set,[12] the 6-31G split valence basis set,[13] the standard Dunning double-ζ (DZ) basis set—a 4s/2p contraction[14,15] of the 9s/5p primitive set of Huzinaga[16] on carbon and the corresponding unscaled 4s/2s contraction on hydrogen—and a double-ζ plus polarization (DZP) basis set with polarization exponents of 0.75 on both carbon and hydrogen.

The basis sets are split up among the 15 atoms as follows: the four carbon atoms and the two hydrogen atoms directly involved in the abstraction have one basis set (bs1), while the nine remaining hydrogen atoms, the ones that would be carbon atoms in diamond, share a second basis set (bs2). We denote the total basis set bs1/bs2. Table I shows the basis set dependence of the reaction energy calculated at the Hartree–Fock level not including zero-point vibrational energy corrections. The four basis sets included in the comparison are 6-31G/STO-3G, 6-31G/6-31G, DZ/DZ, and DZP/DZ. All structures are completely optimized at the respective levels of theory. The results show that the reaction energy is quite insensitive to the basis set for the basis sets considered; the most modest basis set (6-31G/STO-3G) and the most extensive (DZP/DZ) differ by only 0.6 kcal/mol in their prediction of the reaction energy. On the basis of this insensitivity, we choose to use

Table I. Basis Set Dependence of the Hartree–Fock Energy Difference for $(CH_3)_3CH + H \rightarrow (CH_3)_3C + H_2$

bs1/bs2	N^a	energy, hartrees $(CH_3)_3CH + H$	energy, hartrees $(CH_3)_3C + H_2$	ΔE, kcal/mol
6-31G/STO-3G	49	−157.6866	−157.6895	1.7
6-31G/6-31G	58	−157.7337	−157.7374	2.3
DZ/DZ	62	−157.7498	−157.7536	2.4
DZP/DZ	92	−157.8178	−157.8214	2.3

[a] Number of contracted basis functions.

Table II. MCSCF Structural Parameters[a] for Gas-Phase Hydrogen Atom Abstraction from Isobutane

	$(CH_3)_3CH + H$	$(CH_3)_3C - H - H$	$(CH_3)_3C^{\bullet} + H_2$
R_p	0.468	0.374	0.226
R_{CC}	1.535	1.521	1.508
R_{CH}	1.111	1.349	∞
R_{HH}	∞	0.991	0.753
$R_{CH'}$	1.088	1.088	1.088
$R_{CH''}$	1.089	1.091	1.093
$\angle_{CCH'}$	111.24	111.26	111.28
$\angle_{CCH''}$	110.87	110.79	110.80
$\angle_{HCCH''}$	60.1	60.2	60.0

[a] Angstroms and degrees.

(9) Siegbahn, P. E. M.; Heiberg, A.; Roos, B. O.; Levy, B. *Phys. Scr.* **1980**, *21*, 323.
(10) Roos, B. O.; Taylor, P. R.; Siegbahn, P. E. M. *Chem. Phys.* **1980**, *48*, 152.
(11) MESA (Molecular Electronic Structure Applications), P. Saxe, B. H. Lengsfield, R. Martin, and M. Page.
(12) Hehre, W. J.; Stewart, R. F.; Pople, J. A. *J. Chem. Phys.* **1969**, *51*, 2657.
(13) Hehre, W. J.; Ditchfield, R.; Pople, J. A. *J. Chem. Phys.* **1972**, *56*, 2657.
(14) Dunning, T. H., Jr. *J. Chem. Phys.* **1970**, *53*, 2823.
(15) Dunning, T. H.; Hay, P. J. Methods of Electronic Structure Theory. In *Modern Theoretical Chemistry*; Schaefer, H. F., III, Ed.; Plenum Press: New York, 1977; Vol. 3.
(16) Huzinaga, S. *J. Chem. Phys.* **1965**, *42*, 1293.

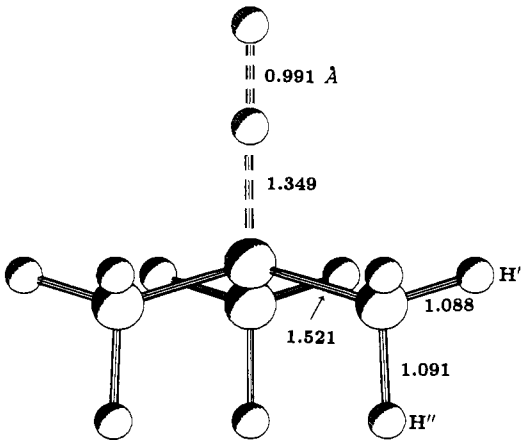

Figure 1. MCSCF structure of the transition state for the gas-phase hydrogen abstraction from isobutane by a hydrogen atom. The CH and HH bonds being broken and formed in the reaction are stretched by about 21% and 18% from their respective equilibrium values.

the 6-31G/STO-3G basis set for subsequent MCSCF calculations of features of the transition-state region. At the MCSCF level, and with zero-point vibrational energy corrections included, the calculated 0 K enthalpy of reaction is within 2 kcal/mol of experiment.

IV. Complete Radical Relaxation: The Gas-Phase Abstraction Reaction

Structures for the reactant isobutane, the product *tert*-butyl radical, and the abstraction transition state connecting these two species have been fully optimized at the 3-in-3 CASSCF 6-32G/STO-3G level of theory. Although all structures have been optimized assuming no elements of symmetry, we find that all three structures possess C_{3v} symmetry. The structural parameters are presented in Table II and, where ambiguous, are defined according to the atom labels in the gas-phase transition state shown in Figure 1. Harmonic vibrational frequencies and resulting zero-point vibrational energies for all three species are reported in Table III. The calculated structure of isobutane agrees well with the experimental microwave structure of Lide[17] and with the theoretical structure reported by Yoshimine and Pacansky.[18] The first parameter in Table II, R_p, is a measure of the degree of pyramidalization about the central carbon atom; it is the distance between the central carbon atom and the plane formed by the other three carbon atoms. The gas-phase structure of the *tert*-butyl radical (R_p = 0.226 Å) is about halfway between the nearly tetrahedral isobutane (R_p = 0.468 Å) and a planar arrangement of the four carbon atoms (R_p = 0.0 Å). The length of the breaking CH bond at the transition state (1.349 Å) is 21.3% greater than its value in isobutane (1.111 Å), while the HH bond is extended by 18.3% over its final value in H_2. The transition state is thus fairly centrally located as it should be for a nearly thermoneutral reaction.

The *tert*-butyl radical is stabilized by a *hyperconjugation* interaction.[19] This is a resonance interaction (three of them can be drawn here) in which the radical electron in a p-type orbital on the central carbon atom interacts with an adjacent CH bond that is aligned with it. This gives partial double bond character to the CC bonds and weakens the CH″ bonds. Several features in Tables II and III support such a resonance stabilization. First, the CC bonds shorten from 1.535 Å in isobutane to 1.508 Å in the *tert*-butyl radical and have a length at the transition state about halfway between these values, consistent with increasing double bond character with increased radical character. Second, the CH″ bonds lengthen from 1.089 Å at isobutane to 1.091 Å at the transition state to 1.093 Å at the *tert*-butyl radical, while the CH′ bond lengths do not change. Finally, of the nine CH stretch normal vibrational modes, the six of them that have substantial CH″ character all have frequencies that are reduced by 20–30 cm^{-1} from isobutane to *tert*-butyl radical, while the three modes that do not involve CH″ stretches remain the same.

Table III. MCSCF Harmonic Vibrational Frequencies (cm^{-1}) for Gas-Phase Hydrogen Atom Abstraction from Isobutane

	$(CH_3)_3CH + H$	$(CH_3)_3C - H - H$	$(CH_3)_3C^{\bullet} + H_2$
		2029i	
		185	
	209	229 (2)	
	264 (2)	329 (2)	101
	399 (2)	404 (2)	141 (2)
	474	442	296
	848	823	404 (2)
	1021 (2)	1040 (2)	801
	1065	1075	1052 (2)
	1056 (2)	1093 (2)	1079
	1315 (2)	1195	1103 (2)
	1473 (2)	1279 (2)	1247
	1364	1418 (2)	1422 (2)
	1586 (2)	1430	1591 (2)
	1612	1586 (2)	1614
	1670	1610	1667
	1680 (2)	1664	1669 (2)
	1689 (2)	1672 (2)	1683 (2)
	1697	1682 (2)	1683
	2937	1690	3170 (2)
	3190 (2)	3182 (2)	3174
	3194	3187	3244 (2)
	3274	3262 (2)	3248
	3274 (2)	3266	3270
	3278 (2)	3278	3275 (2)
	3280	3282 (2)	4255
ZPE[a]	88.8	86.9	85.8

[a] Zero-point vibrational energy (kcal/mol).

The calculated MCSCF (6-31G/STO-3G) activation barrier is about 8 kcal/mol too high as compared to experiment. This difference is expected given the modest basis set and, probably more importantly, the neglect of dynamical electron correlation. However, because we are interested in *changes* in energies accompanying geometric constraints, the absolute value of the barrier height is of little concern. Instead, it is the reaction energy that is important here because the reaction energy determines the location of the transition state and, consequently, the degree of radical character at the transition state. The calculated reaction energy, −6.7 kcal/mol, is close to the experimental value of −8.4 kcal/mol.

V. Limited Radical Relaxation

a. A Hypothetical *Bulk Terminated* Reaction. We can put a limit on the effect of the diamond lattice geometrical constraints on the structures and energetics of the abstraction reaction by examining the potential energy surface for a hypothetical case in which no radical relaxation is allowed. Here we begin with the near tetrahedral isobutane and abstract a hydrogen like in the gas-phase case, but this time the transition state is located in the reduced space of only the lengths of the breaking CH bond and forming HH bond. The completely unrelaxed product radical is 5.4 kcal/mol higher in energy than the fully relaxed radical. Thus, in the absence of any surface radical relaxation, the strength of any surface CX bond would be 5.4 kcal/mol greater than a corresponding gas-phase tertiary CX bond.

Because the reaction exothermicity is reduced by the geometrical constraints, the transition state is shifted toward the reactant; the CH bond at the *bulk terminated* transition state is 0.04 Å longer and the HH bond is 0.04 Å shorter than the corresponding gas-phase values. Also, the activation energy for abstraction is increased by 1.7 kcal/mol from the gas-phase value.

b. Partial Relaxation: Abstraction from Diamond. While the *bulk terminated* reaction may put an upper limit on the effect of lattice constraints on the abstraction reaction, it is not necessarily a good model for diamond. In diamond, the immediate structure around the radical site can make an effort to relax toward the

(17) Lide, D. R. *J. Chem. Phys.* **1960**, *33*, 1514.
(18) Yoshimine, M.; Pacansky, J. *J. Chem. Phys.* **1981**, *74*, 5168.
(19) Morrison, R. T.; Boyd, R. N. *Organic Chemistry*; Allan and Bacon: Boston, 1973; p 216.

Table IV. Key Structural Parameters (Å) for the Constrained Abstraction Reaction

	transition state			radical
	R_p	R_{CH}	R_{HH}	product R_p
gas-phase	0.374	1.349	0.991	0.225
bulk terminated	0.468	1.389	0.950	0.468
partially relaxed	0.386	1.353	0.987	0.286

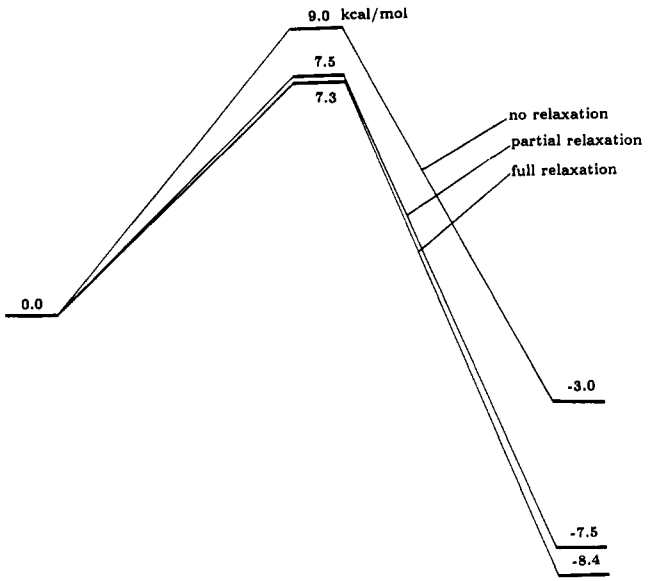

Figure 2. Energetics for the hydrogen atom abstraction from isobutane, from isobutane constrained to disallow radical relaxation, and from isobutane partially constrained to model a diamond lattice. The bottom curve (full relaxation) is adjusted to correspond to known gas-phase energetics. The two other curves represent the effect of structural constraints calculated at the MCSCF level of theory.

gas-phase structure. However, this effort is thwarted by the energetic cost of disrupting the neighboring structure, and the true structures and energetics result from a compromise between these two effects.

As a situation closer to the limited radical relaxation allowed in diamond, we perform constrained calculations of the abstraction pathway allowing the central carbon atom to relax in the field of its fixed neighbors at each stage of the reaction. This situation is between the gas-phase and *bulk terminated* extremes but still underestimates the full relaxation available to a diamond lattice because neighboring carbon atoms are not allowed to relax. Thus our partially relaxed calculations still represent an upper limit on the effect of geometrical constraints on the abstraction reaction.

The results for the geometrical parameters are given in Table IV, and the energetics for all three cases are summarized in Figure 2. The unconstrained (full relaxation) energetics shown in Figure 2 are known gas-phase experimental numbers. The activation energy (7.3 kcal/mol) is the generic value recommended for abstraction of tertiary hydrogen atoms by atomic hydrogen for use in combustion modeling.[20] The MCSCF calculations then provide the *difference* between the fully relaxed and the various constrained energetics. The results—surprisingly to us—are that most (85%) of the available 5.4 kcal/mol of relaxation energy for the product radical is realized by allowing only the radical carbon atom, and not any of its neighbors, to move. In fact, without allowing the three neighboring carbon atoms to move, the radical carbon atom nevertheless goes almost as far toward a planar (sp^2) arrangement as does the gas-phase radical. The radical carbon atom essentially *sinks down* into the fixed framework of the neighboring carbon atoms, accepting the consequently shorter CC bond lengths. The negative consequences of this CC bond shortening are small, however, because as shown by the gas-phase structural parameters in Table II, the radical actually wants shorter CC bonds as a reflection of a hyperconjugative resonance interaction.

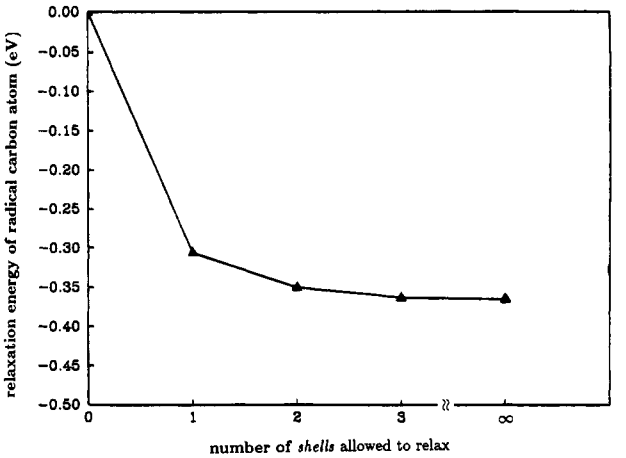

Figure 3. Energetic effect of structural relaxation for a lone carbon radical site on a hydrogenated diamond {111} surface calculated by using an empirical Tersoff-type potential. The origin of the plot corresponds to a hydrogenated diamond surface with one hydrogen atom removed but with no subsequent relaxation of the radical site. Relaxation energy is plotted against the number of *shells* of carbon atoms allowed to relax. One shell corresponds to relaxation of only the radical carbon atom; two shells corresponds to relaxation of the radical carbon atom and its three near neighbors, etc.

The results for the transition-state structure and the activation energy are also dramatic. The structural parameters for the transition state with partial relaxation are very close to those for the gas-phase transition state. For example, in the gas phase, the central carbon atom sinks down by 0.094 Å from the reactant isobutane to the transition state, while for the partially relaxed transition state, the central carbon atom sinks down into the plane of the other three carbon atoms by nearly as much, by 0.082 Å. The CH and HH bond lengths at the partially relaxed transition state, given in Table IV, are also much closer to the gas-phase transition-state bond lengths than they are to the bulk terminated bond lengths. Finally, the activation energy for the partially relaxed reaction is only 0.2 kcal/mol higher than the activation energy for the gas-phase reaction.

VI. Full Radical Relaxation in Diamond from an Empirical Potential

The primary result of our ab initio calculations is that most of the structural and energetic relaxation effects for a surface carbon radical are realized by motion of only that carbon atom. This conclusion comes from comparing calculations of the unconstrained *tert*-butyl radical to calculations of the *tert*-butyl radical with all atoms but the central carbon atom constrained to keep the structure they had in isobutane. The assumption is that the electronic structure about the central carbon atom is independent of whether its second neighbors are hydrogen atoms or carbon atoms. Given this assumption, the maximum effect of radical relaxation for diamond is the relaxation found for the gas-phase *tert*-butyl radical.

Although it is impractical to do with ab initio calculations, we can use an empirical Tersoff-type potential for diamond[21] to model a large enough cluster to study the convergence of radical relaxation with the number of carbon neighbors allowed to relax. We begin with a fully hydrogenated diamond {111} surface. We then remove a hydrogen atom without allowing any structural relaxation. Figure 3 shows the radical relaxation energy as a function of the number of *shells* of neighboring carbon atoms allowed to relax. One shell corresponds to relaxation of only the central carbon atom, as in the ab initio calculations. Two shells corresponds to relaxation of the central carbon atom and the next

(20) Westbrook, C. K.; Warnatz, J.; Pitz, W. J. *Twenty Second Symposium (international) on Combustion*; The Combustion Institute, 1988; p 893.

(21) Brenner, D. W. *Phys. Rev. B* **1990**, *42*, 9458.

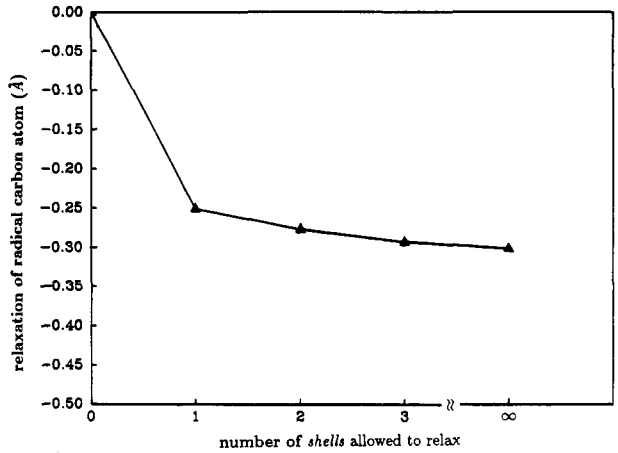

Figure 4. Same as Figure 3 except that the vertical relaxation distance of the radical carbon atom instead of relaxation energy is now plotted against the number of shells of carbon atoms allowed to relax.

three carbon atoms, etc. Figure 4 is the corresponding plot for the pyramidalization about the radical center.

Although the absolute magnitude of the energetic and structural effects of radical relaxation is about 50% larger for the empirical potential, the results are consistent with the ab initio calculations in that most of he energetic and structural effects of radical relaxation result from motion of only the radical carbon atom itself. The effect converges rapidly after the first carbon atom and collectively contributes only about another 10–15% to the radical relaxation.

VII. Conclusions

The radical generated by removing a hydrogen atom from hydrogenated diamond {111} is able, despite the constraints imposed by the surrounding lattice, to relax nearly to the extent that it does in the gas phase. This, in part, is because the radical is willing to accept shorter CC bond lengths and can therefore sink down toward planarity without disturbing the surrounding lattice. Thus bond strengths to surface carbon atoms should be similar to (about 1 kcal/mol greater than) bond strengths to gas-phase tertiary carbon atoms. Furthermore, this analysis holds for the transition states for abstraction reactions as well; the constraints of the lattice have little effect on the barriers for hydrogen abstraction reactions. We calculate an increase in the activation energy of only 0.2 kcal/mol when the structure surrounding a tertiary carbon atom is constrained similar to the way it is in a diamond lattice as compared to an unconstrained gas-phase reaction. Therefore, in kinetic modeling or molecular dynamics simulations of diamond film growth, the use of activation energies for surface hydrogen abstraction reactions taken from analogous gas-phase hydrocarbon reactions with minimal or no adjustment is justified.

Acknowledgment. This research was supported by the Office of Naval Research through the Naval Research Laboratory.

Registry No. H_2, 12385-13-6; $(CH_3)_3CH$, 75-28-5; diamond, 7782-40-3.

Heteronuclear Diatomic Metal Cluster Ions in the Gas Phase: Theoretical Treatment of $MgFe^+$ and Study of Its Reactions with Hydrocarbons

Lisa M. Roth,[†] Ben S. Freiser,*[,†] Charles W. Bauschlicher, Jr.,[‡] Harry Partridge,[‡] and Stephen R. Langhoff[‡]

Contribution from the Department of Chemistry, Purdue University, West Lafayette, Indiana 47907, and NASA Ames Research Center, Moffett Field, California 94035.
Received July 2, 1990. Revised Manuscript Received October 29, 1990

Abstract: The unique reactivity of $MgFe^+$ is described. This cluster reacts with linear alkenes (C_2–C_6) by displacement of magnesium to form an Fe^+–olefin product. In contrast, $MgFe^+$ reacts with alcohols by displacement of the iron to form a Mg^+–alcohol product. This is the first example of a changeover in the relative metal–ligand bond energies with both metals in a dimer being selectively displaced. $MgFe^+$ also reacts with cyclic alkenes. For example, it dehydrogenates cyclohexene to form $MgFe^+$–benzene, which reacts further to displace the magnesium and form benzene–Fe^+–cyclohexene. $MgFe^+$ is unreactive with small alkanes (C_2–C_4) but reacts with larger alkanes (C_5–C_7) to form a $MgFe^+$–alkene product. An upper limit of 34 ± 5 kcal/mol for $D°(Mg^+–Fe)$ has been established by use of ion–molecule reactions. In contrast, the photodissociation threshold for $MgFe^+$ to form Fe^+ yields an upper limit of $D°(Mg^+–Fe) \leq 44 \pm 3$ kcal/mol. Theoretical calculations show that $MgFe^+$ has a $X^6\Delta$ ground state and bonds by forming a covalent Fe(4s)–Mg(3s) bond. The computed binding energy of 29.4 kcal/mol, which is expected to be a lower bound, is consistent with the upper limit determined from ion–molecule reactions. The calculations show that the photon absorption at ≃49 kcal/mol corresponds to the intense $(2)^6\Delta \leftarrow X^6\Delta$ transition. This explains the large difference between the dissociation energy deduced from the ion–molecule reactions and the upper bound determined from photodissociation.

Introduction

The gas-phase chemistry of atomic metal ions and small metal cluster ions continues to be of great interest.[1] These systems provide information that can be applied to a wide range of disciplines, including surface science, catalysis, and atmospheric chemistry. For example, magnesium and iron have been detected in the atmosphere by airborne mass spectrometers. These metals are introduced by meteor ablation and have been observed in the 100-km-altitude region.[2] Several laboratory studies have been

[†] Purdue University.
[‡] NASA Ames Research Center.

(1) Morse, M. D. *Chem. Rev.* **1986**, *86*, 1049.

0002-7863/91/1513-3274$02.50/0